

Published in final edited form as:

*Nanomedicine (Lond)*. 2014 August ; 9(12): 1807–1820. doi:10.2217/nnm.14.44.

## Nanomicelle formulation modifies the pharmacokinetic profiles and cardiac toxicity of daunorubicin

Hongyong Zhang<sup>1</sup>, Yuanpei Li<sup>2</sup>, Tzu-yin Lin<sup>1</sup>, Kai Xiao<sup>2</sup>, Ashraf S Haddad<sup>3</sup>, Paul T Henderson<sup>1</sup>, Brian A Jonas<sup>1</sup>, Mingyi Chen<sup>4</sup>, Wenwu Xiao<sup>2</sup>, Ruiwu Liu<sup>2</sup>, Kit S Lam<sup>1,2</sup>, and Chong-xian Pan<sup>\*,1,3,5</sup>

<sup>1</sup>Division of Hematology & Oncology, Department of Internal Medicine, School of Medicine, University of California, Davis, 4501 X Street, Room 3016, Sacramento, CA 95817, USA

<sup>2</sup>Department of Biochemistry & Molecular Medicine, School of Medicine, University of California, Davis, Sacramento, CA 95817, USA

<sup>3</sup>Department of Urology, University of California, Davis Comprehensive Cancer Center, Sacramento, CA 95817, USA

<sup>4</sup>Department of Pathology, University of California, Davis, Sacramento, CA 95817, USA

<sup>5</sup>Veterans Affairs Northern California Health Care System, 10535 Hospital Way, Mather, CA 95655, USA

### Abstract

**Background**—Treatment with daunorubicin (DNR) in acute myeloid leukemia is moderately effective and associated with significant side effects, including cardiac toxicity. We recently developed a nanomicellar formulation of DNR that specifically targets acute myeloid leukemia stem cells.

**Materials & methods**—Pharmacokinetics analysis of free DNR, DNR in nanomicellar formulations was performed in Balb/c mice and Sprague–Dawley rats. Histochemical staining, caspase 3/7, troponin and creatine kinase MB isoenzyme were used to assess toxicity.

**Results**—Compared with free DNR, the nanomicellar formulations of DNR had less cardiotoxicity as evidenced by milder histopathological changes, lower caspase 3/7 activity in heart tissue ( $p = 0.002$ ), lower plasma creatine kinase MB isoenzyme ( $p = 0.002$ ) and troponin concentrations ( $p = 0.001$ ) postinjection. The area under curve concentration of DNR in micelles increased by 31.9-fold in mice ( $p < 0.0001$ ) and 22.0-fold higher in rats ( $p < 0.001$ ).

---

\* Author for correspondence Tel.: +1 916 734 3771, Fax: +1 916 734 7946, cxpan@ucdavis.edu.

#### Financial & competing interests disclosure

The authors have no other relevant affiliations or financial involvement with any organization or entity with a financial interest in or financial conflict with the subject matter or materials discussed in the manuscript apart from those disclosed.

No writing assistance was utilized in the production of this manuscript.

#### Ethical conduct of research

The authors state that they have obtained appropriate institutional review board approval or have followed the principles outlined in the Declaration of Helsinki for all human or animal experimental investigations. In addition, for investigations involving human subjects, informed consent has been obtained from the participants involved.

**Conclusion**—Leukemia stem cell-targeting micelles dramatically change the pharmacokinetics and reduce the cardiac toxicity of DNR, which may enable improved DNR-based treatment of acute myeloid leukemia.

### Keywords

cardiotoxicity; daunorubicin; leukemia stem cells; nanomicelles; pharmacokinetics

For most patients with acute myeloid leukemia (AML), the 3 + 7 regimen, with 3 days of an anthracycline and 7 days of cytarabine, is still the standard first-line chemotherapy. This regimen is only moderately effective. The overall long-term survival for young patients (<60 years) is less than 30%. It is less than 10% for elderly patients. The prognosis of AML has not changed significantly over the last three decades. This regimen is associated with significant toxicity even with intensive monitoring and supportive care at the inpatient setting. One of the major side effects of anthracyclines is cardiac toxicity. This is especially true with AML as the median age of diagnosis is approximately 65 years, and many of these patients already have risk factors for cardiovascular diseases. Various approaches have been adopted to decrease the cardiac toxicity. Nanoparticles, such as liposomes [1], polymer micelles [2,3] and dendrimers [4], are effective carriers to deliver many kinds of anticancer drugs. Liposomal encapsulation of anthracycline, especially doxorubicin, is associated with significant decrease in heart failure and cardiac damage, but equivalent efficacy for several cancer types [5–7].

We previously reported the development of a novel micelle-based daunorubicin (DNR) nanoformulation that features decoration of the nanoparticle surface with a ligand targeting the CLL1, which is expressed on the acute myeloid leukemia stem cells' (LSCs) surface [8]. These micelles are made of polymers named telodendrimers that have a polyethylene glycol (PEG) backbone conjugated to amphiphasic cholic acid through lysine at one terminus, and CLL1-targeting peptide (amino acid sequence: CDLRSAAVC) at the other terminus of the PEG (Figure 1A). The amphiphilic nature of telodendrimers enables them to self-assemble in solution to form nanometer-size micelles that can sequester drugs such as DNR in the interior [2,3,9].

One unique advantage of this micellar formation is that the CLL1-targeting ligand confers specific drug delivery into LSCs, while sparing normal hematopoietic stem cells [8,10,11]. LSCs are a special group of leukemia cells that express some of the same cell surface markers as normal hematopoietic stem cells, possess the stem cell features of self-renewal and generation of more differentiated leukemic cells [12,13]. LSCs are relatively chemoresistant, can survive conventional chemotherapy and subsequently generate more leukemic cells resulting in disease recurrence. In order to cure leukemia, LSCs must be eradicated [14–16]. We previously demonstrated that the CLL1-targeting ligand could not only attach the micelles to the surface of cells expressing CLL1, but, more importantly, induce uptake of the whole micelles together with the drug load into the target cells [8].

Another advantage of targeting leukemia via micelles is that leukemic cells and LSCs are located in bone marrow and blood vessels that are in direct contact with micelles after intravenous injection. PEG on the surface decreases nonspecific uptake by other cells, while

the CLL1-targeting ligand guides cell-specific delivery of the drug load into LSCs. In addition, after DNR is released into blood circulation, it can kill leukemic cells throughout the body. DNR is a small molecule (molecular weight: 527.5 Da) and relatively hydrophobic, so it diffuses into tissue rapidly ( $T_{1/2\alpha}$ : ~2 min) after intravenous administration with large volume of distribution (40 l/kg). Nanoformulation of DNR encapsulates DNR in micelles with an approximate size of 14 nm that significantly restricts the tissue distribution of DNR. The loading ratio of our micellar formulation is 25% (weight/weight of DNR/micelle). Based on our calculation, there are approximately 430 DNR molecules per micelle. The main objective of this study was to determine whether micellar formulation of DNR significantly modifies the pharmacokinetics (PKs) of DNR in favor of increased drug exposure of leukemic cells with reduced cardiac toxicity compared with free DNR.

## Materials & methods

### Materials

DNR was purchased from Merck Millipore (MA, USA). Monomethyl-terminated PEG monoamine (MeO-PEG-NH<sub>2</sub>; molecular weight: 5 kDa) was purchased from Rapp Polymere (Tübingen, Germany). Fmoc-lysine(Fmoc)-OH was purchased from NeoMPS Inc. (CA, USA). A, Cremophor<sup>®</sup> EL, hexynoic acid, trifluoroacetic acid and tetrakis (triphenylphosphene) palladium(0) [Pd(Ph<sub>3</sub>P)<sub>4</sub>] and phenylsilane were purchased from Sigma-Aldrich (MO, USA). Rink amide resin, Fmoc-lysine(Alloc), 6-Cl-HOBt and all Fmoc-amino acids were purchased from AAPPTec (KY, USA). Chronic myelogenous leukemia cells K562 was purchased from American Type Culture Collection (MA, USA); K562-CLL1 cells were obtained by infecting K562 cells with a lentivirus vector expressing *CLL1* gene.

### Synthesis of CLL1-targeting peptide

The methodology to synthesize CLL1-targeting peptide has been described previously (Supplementary Information 1, see online at [www.futuremedicine.com/doi/suppl/10.2217/nmm.14.44](http://www.futuremedicine.com/doi/suppl/10.2217/nmm.14.44)) [8,17]. In brief, a Fmoc-lysine(Alloc) was coupled onto the amino group on Rink amide resin. The amino group on the side chain of lysine was used to introduce alkyne for the postcleavage conjugation of CLL1-targeting peptide to the telodendrimer molecule. The peptide was synthesized on the N-terminal of lysine(Alloc)-Rink resin sequentially via Fmoc peptide chemistry [18]. Then hexynoic acid was coupled onto the lysine side chain after removal of Alloc with Pd(Ph<sub>3</sub>P)<sub>4</sub> in the presence of phenylsilane. After the peptide-lysine (alkyne) was cleaved from the solid support with trifluoroacetic acid cocktail (phenol/thioanisole/H<sub>2</sub>O/EDT/ trifluoroacetic acid (0.75:0.5:0.5:0.25:10, weight/volume/volume/volume/volume), the crude peptide was cyclized via the oxidative disulfide formation of the two cysteines located at the flank of the peptide. Crude peptide was purified by reverse-phase HPLC to at least 95% purity. The purity of the resulting peptides was determined by analytical HPLC. MALDI-TOF mass spectrometry was used to confirm the identity of the peptide.

## Synthesis of telodendrimers

The synthesis of PEG<sup>5k</sup>-CA<sub>8</sub> telodendrimers was performed as previously reported in which eight cholic acid units were conjugated to PEG (Supplementary Information 2) [2]. In brief, PEG<sup>5k</sup>-CA<sub>8</sub> was synthesized via solution phase condensation reactions from MeO-PEG-NH<sub>2</sub> with a molecular weight of 5000 Da. Fmoc-lysine(Fmoc)-OH (2 equivalents) was coupled onto the amino group on PEG using 6-chloro-1-hydroxybenzotriazole (6-Cl-HOBt) and diisopropylcarbodiimide as activating reagents. The completion of the coupling was monitored by Kaiser test. The di-Fmoc-PEG was precipitated by adding cold diethyl ether and washed with ether twice. The two Fmoc groups were removed by the treatment with 20% piperidine in dimethylformamide, and the resulting di-amine-PEG was precipitated, washed three-times by cold ether, and dried under vacuum. Two repeated couplings of Fmoc-lysine(Fmoc)-OH and Fmoc-deprotection were carried out to generate a third generation of dendritic polylysine on one terminus of PEG. Cholic acid N-hydroxysuccinimide ester was coupled to the terminal end of dendritic polylysine, resulting in PEG<sup>5k</sup>-CA<sub>8</sub>. This telodendrimer was subsequently dialyzed and lyophilized to yield a white powder.

CLL1-targeting telodendrimers were synthesized based on the method reported previously [8]. Briefly, Cu(I)-catalyzed click chemistry was used for coupling the alkyne group of CLL1-targeting peptides onto the azide groups at the end of PEG on the telodendrimer in aqueous phase. The purity of the CLL1-targeting telodendrimer was analyzed using HPLC, and the molecular weight was measured by MALDI-TOF mass spectrometry.

## Preparation & characterization of DNR-loaded nontargeting & CLL1-targeting micelles

The 'dry-down' method was used for DNR loading [9]. To synthesize nontargeting DNR-loaded micelles (NTM-DNR), telodendrimers (PEG<sup>5k</sup>-CA<sub>8</sub>) were used, while telodendrimers (PEG<sup>5k</sup>-CA<sub>8</sub>) and CLL1-telodendrimers (CLL1-PEG<sup>5k</sup>-CA<sub>8</sub>) at 1:1 ratio were used to synthesize CLL1-targeting micelles loaded with DNR (CTM-DNR). DNR and telodendrimers were dissolved in chloroform, and evaporated in rotavapor to obtain a dry polymer–drug film. The film was reconstituted in phosphate-buffered saline (PBS), followed by sonication for 2 h, allowing the polymer to self-assemble into DNR-loaded micellar nanoparticles. The micelle solution was filtered with a 0.22 μm filter to sterilize the sample. The final product was analyzed for drug-loading capacity by HPLC analysis, for size and size distribution with a dynamic light scattering (Microtrac, PA, USA) and transmission electron microscopy (Philips CM-120; Philips Research, NY, USA).

## Animals

Male BALB/c mice (10–12 weeks of age), male nude mice (6–8 weeks of age) and male Sprague–Dawley rats with jugular vein catheters (body weight: 200 to ~250 g) were both purchased from Harlan (CA, USA). All animals were kept under pathogen-free conditions according to the Association for Assessment and Accreditation of Laboratory Animal Care International guidelines and were allowed to acclimatize for at least 4 days prior to any experiments. All animal experiments were performed in compliance with institutional guidelines and according to protocol number 16273 approved by the Animal Use and Care Administrative Advisory Committee at the University of California, Davis (CA, USA).

## PKs & biodistribution in mice & rats

Three groups of three BALB/c mice or rats received a single intravenous injection 10 mg/kg (mice) or 5 mg/kg (rats) body weight of free DNR, DNR-loaded nontargeting (NTM–DNR) or CLL1-targeting micelles (CTM–DNR). To prevent crosscontamination, drugs were administered through the tail vein, while blood specimens were sampled through the jugular vein catheter. Animals receiving drug-free telodendrimers served as control. Blood was collected at different time points (0, 1, 3, 5, 15 and 30 min, 1, 2, 4, 8 and 24 h postinjection) in EDTA tubes, and plasma was separated by centrifugation and kept at  $-20^{\circ}\text{C}$  until analysis. In total, 10  $\mu\text{l}$  of plasma were added to 190  $\mu\text{l}$  of extraction buffer (10% Triton<sup>TM</sup> X-100, Sigma-Aldrich; deionized water, and acidified isopropanol (0.75 N HCl) with 1:2:15 volumetric ratio), and DNR was extracted overnight at  $-20^{\circ}\text{C}$ . Standard curves for DNR drug in blood were drawn by the addition of free DNR to whole blood using the same centrifugation, extraction and quantification protocols. The fluorescence of the supernatant was determined at excitation/emission of 470 nm/590 nm. Plasma DNR concentration was measured and compared with a standard curve of DNR concentration prepared in the same plasma–micelle matrix. The parameter profiles of PK studies were calculated and analyzed by using Kinetica Trial Version 5.0 (Adept Scientific Ltd, London, UK).

At 24-h postinjection, major organs (heart, liver, spleen, lung and kidney) were harvested. Tissues (100 mg) were mixed with 900  $\mu\text{l}$  extraction buffer, and homogenized using POLYTRON<sup>®</sup> PT 10–35 homogenizer (Kinematica AG, Littau/Lucerne, Switzerland). DNR was extracted overnight at  $-20^{\circ}\text{C}$  using the same method described above. To eliminate the intrinsic background fluorescence signal, organs from mice not treated with drugs were used as blank controls. The samples were centrifuged at 3000 rpm for 5 min after mixing, and the supernatant was used for the fluorescence measurement. Sample recovery standard curves for each tissue were generated by mixing a range of free DNR concentrations with each homogenized tissue type followed by the same extraction and quantification procedure. The biodistribution data were expressed as the actual concentration of DNR and its metabolites per gram tissue.

## Histological analysis & determination of cardiac toxicity

For histological evaluation, vital organs were fixed in 10% formalin followed by paraffin embedding and sectioning performed in the Veterinary Medical Teaching Hospital at University of California, Davis. Tissue sections were stained by hematoxylin and eosin stain and examined under a light microscope. Plasma samples were isolated from experimental animals and tested with a creatine kinase MB isoenzyme (CK-MB) ELISA kit and a cardiac troponin T (cTnT) ELISA kit (Mybiosource, CA, USA). A Caspase-Glo<sup>®</sup> 3/7 assay kit (Promega, WI, USA) was used to measure the level of Caspase 3/7 in heart tissues per manufacturer's instruction. The plasma and heart tissues from the mice injected with PBS alone were used as a control.

## Efficacy of CTM loaded with DNR in mice bearing K562-CLL1 xenograft

Male nude mice bearing K562-CLL1 were created by subcutaneous injection of 100  $\mu\text{l}$  of K562-CLL1 at a density of  $1.0 \times 10^7$  cells/ml suspended in PBS. When the xenografts reached the size of approximately 200  $\text{mm}^3$ , mice were treated with free DNR (10 mg/kg),

or CTM–DNR at low dose (10 mg/kg) and high dose (20mg/kg), respectively, or PBS as the control at 1, 3, 6, 9, 12, 15 and 18 days by tail vein. Tumor growth was evaluated by measuring the tumor volume (length × width × width/2) once every 3 days.

### Statistical analysis

Since the primary purpose is to determine the degree of exposure following administration of a drug (such as area under the concentration curve [AUC]), and the drug's associated PK parameters, such as clearance, elimination half-life,  $T_{max}$  and  $C_{max}$ , among others, noncompartmental analysis is usually the preferred methodology that was used during the PK analysis [19]. PK studies were analyzed using the Kinetica Trial Version 5.0. Statistical analysis was performed by using GraphPad InStat™ software (GraphPad Software Inc., CA, USA) and analysis of variance was performed to compare the differences of the three treatment groups. All results were expressed as the mean ± standard error unless otherwise noted. A value of  $p < 0.05$  was considered statistically significant.

## Results

### Comparison of PK & biodistribution of DNR in mice

Two types of micelles, both loaded with DNR, were synthesized for this study: nontargeting micelles (NTM–DNR) and CLL1-targeting micelles (CTM–DNR). The critical micellar concentrations for targeted and nontargeted micelles were comparable, 0.011 mg/ml for targeted micelles and 0.017 mg/ml for nontargeted micelles, respectively. To determine if micellar formulations of DNR changed the PKs, blood specimens were obtained at different time points after a single injection of free DNR, NTM or CTM at a dose of 10 mg/kg of DNR. Based on the PK data (Figure 2 & Table 1), the concentrations of the injected CTM–DNR and NTM–DNR were much greater than their critical micellar concentration. All three formulations of DNR had a characteristic first phase of rapid tissue distribution and decline of plasma DNR concentration. However, free DNR was much more rapidly cleared from the plasma with an initial half-life in plasma of  $1.11 \pm 0.04$  min ( $T_{1/2\alpha}$ ), compared with  $5.93 \pm 2.76$  min ( $p = 0.02$ ) with NTM–DNR and  $11.63 \pm 6.37$  min ( $p = 0.046$ ) with CTM–DNR (Figure 2A, Table 1 & Supplementary Information 3). After the initial rapid phase, the blood clearance of DNR continued to be cleared at a much faster pace with free DNR with  $T_{1/2\text{kel}}$  of  $0.61 \pm 0.01$  h compared with  $9.08 \pm 0.4$  h (15-fold reduction;  $p < 0.0001$ ) with NTM and  $13.9 \pm 4.15$  h (20-fold reduction;  $p < 0.0001$ ) with CTM. Our analysis did not distinguish free DNR from DNR in micelles since DNR was extracted during analysis. However, free DNR was rapidly cleared from blood, and at any time point, the DNR concentration in the mice treated with free DNR was less than 10% of DNR concentration in mice treated with micellar formations of DNR. Therefore, the prolonged half-lives of CTM and NTM was most likely secondary to the micellar formulation that trapped DNR in blood circulation. The AUC from 0 to 24 h for NTM and CTM were 33.9-fold ( $p < 0.001$ ) and 31.9-fold ( $p = 0.002$ ) greater than free DNR. At 24 h after intravenous administration, the plasma DNR concentration in mice receiving NTM was slightly higher than that in mice receiving CTM ( $419.40 \pm 25.20$  µg/ml vs  $352.33 \pm 31.38$  µg/ml;  $p = 0.02$ ). However, both are much higher than the DNR concentration of  $13.64 \pm 1.92$  µg/ml measured in mice treated with free DNR ( $p < 0.0001$ ).

To determine if the significant modification of PK is reproducible, we performed a similar PK in rats. A similar first rapid decrease of DNR followed by a much slower clearance of DNR was observed in all three formulations. A significant prolongation of half-lives were observed from  $2.01 \pm 1.12$  h with free DNR to  $10.14 \pm 0.99$  h ( $p = 0.0082$ ) with NTM–DNR and  $10.17 \pm 0.54$  h ( $p = 0.0057$ ) with CTM–DNR (Figure 2B & Table 1). The  $AUC_{0-24\text{ h}}$  for NTM and CTM were 25.0-fold ( $p = 0.0056$ ) and 22.0-fold ( $p = 0.0009$ ) higher than free DNR in rats, respectively.

In both cases, the AUC of DNR for CTM–DNR was lower than that of NTM–DNR. This difference was mainly secondary to the initial rapid decrease from tissue distribution. After that initial phase, the clearance of CTM–DNR and NTM–DNR was not statistically significant:  $T_{1/2\beta}$   $31.2 \pm 10$  h with CTM–DNR versus  $20.5 \pm 3$  h with NTM–DNR in mice ( $p = 0.077$ );  $19.20 \pm 1.60$  h with CTM–DNR versus  $16.99 \pm 2.58$  h with NTM–DNR in rats ( $p = 0.080$ ; Table 1).

### Caspase 3/7 induction & plasma biomarkers for cardiomyocyte injury

One major and often the limiting side effect of DNR is cardiac toxicity. Here, we determined whether formulation of DNR in micelles modified the cardiac toxicity. The therapeutic and maximum tolerated dose of DNR is approximately 5–10 mg/kg. It has been reported that liposomal formulation of DNR allows the administration of DNR at three-times the therapeutic dose [20]. We also showed the micellar formulation allows administration of three-times the therapeutic dose without increasing the toxicity in mice [21]. Therefore, we compared the cardiac toxicity of DNR at 15 mg/kg, three-times the therapeutic dose. To determine the extent of cardiac damage, all mice were treated with single dose of DNR at 15 mg/kg. Plasma cardiac damage markers CK-MB and cTnT levels were measured at different time points after dosing. Compared with the control mice, the mice treated with free DNR had much higher plasma CK-MB levels starting at 3 h ( $34.28 \pm 5.77$  U/l vs  $60.02 \pm 4.05$  U/l;  $p = 0.001$ ) after dosing, peaked at approximately 1 day and remained high during 5 days ( $113.98 \pm 10.42$  U/l;  $p = 0.0002$ ) of follow-up. By contrast, the plasma CK-MB levels in the mice treated with DNR in the micellar formulations were no higher than the levels in the control mice, and were much lower than the CK-MB levels of the mice treated with free DNR at all time points ( $p < 0.05$ ; Figure 3A & Supplementary Information 4).

The cTnT levels increased approximately 1 day after treatment. Compared with the cTnT levels in control mice (Figure 3B & Supplementary Information 4), mice treated with free DNR had significant higher cTnT levels starting at 1 day after dosing (9.15-times;  $p = 0.0001$ ), peaking at 3 days (15.8-times;  $p < 0.0001$ ) before decreasing. NTM–DNR and CTM–DNR also induced cTnT, but much lower than the cTnT levels in mice treated with free DNR at all time points ( $p < 0.05$ ). At 1 day after dosing, the cTnT levels were 3.37- (for NTM;  $p = 0.0002$ ) and 3.82-times (for CTM;  $p = 0.0033$ ) higher than the cTnT levels in the control mice, but much lower than the cTnT levels in the mice treated with free DNR (0.37-times;  $p = 0.0006$  for NTM, 0.42-times;  $p = 0.0017$  for CTM). Since both groups of mice treated with the micellar formulations of DNR had decreased levels of CK-MB and cTnT, we concluded that formulation of DNR in micelles, whether there are CLL1-targeting

peptides on the micellar surface or not, could significantly decrease the cardiac toxicity of DNR.

To further characterize the cardiac toxicity, we compared caspase 3/7 induction in cardiac tissue. There was a dose-dependent induction of caspase 3/7 in the groups of mice treated with free DNR (Figure 3C). At 25 mg/kg of free DNR, the caspase 3/7 activity was about 3.46-times than that of the control mice treated with PBS ( $p = 0.001$ ) and was significantly higher than mice treated with 25 mg/kg CTM–DNR ( $p = 0.029$ ). In the groups treated with CTM–DNR, there was no significant increase of caspase 3/7 activity, even at 25 mg/kg, compared with control group ( $p = 0.33$ ), indicating minimal cardiomyocyte apoptosis. These results were in agreement with the histopathologic findings as shown in Figure 4A.

### Histological analysis of organ toxicity

In order to confirm that cardiac toxicity was indeed reduced by micellar formulation, we performed histopathological examination of cardiac tissue and other major organs. Since the cardiac caspase level in mice treated with CTM–DNR at 25 mg/kg was no higher than the mice treated with control (Figure 3C), we compared the histopathological changes of major organs from mice treated with 5 and 25 mg/kg of DNR. In cardiac tissue, 5 days after treatment with free DNR at 25 mg/kg, marked myocardial toxicity was observed and characterized by disarray of cardiomyocytes, disruption or loss of myofibrils and vacuolization of the cytoplasm, patchy necrosis and inflammatory cell infiltration. The histopathological changes in mice treated with CTM–DNR at 25 mg/kg was much less obvious and at a similar degree compared with mice treated with free DNR at 5 mg/kg (Figure 4A).

Moreover, as shown in Figure 4B, DNR-induced liver toxicity with marked zone 3 (perivenal) steatosis hepatitis (fatty liver changes), apoptosis, hyaline globule degeneration at 5 days postinjection of free DNR at both 5 and 25 mg/kg. Minimal histopathological changes were observed in the liver treated with micellar formulation of DNR, especially at 5 mg/kg. Marked red pulp hemorrhage-associated compensative sinusoidal histocytic proliferation and extramedullary hematopoiesis was observed in spleens from mice treated with low- or high-dose free DNR. These toxicities were much more obvious at 25 mg/kg of free DNR. At the therapeutic dose of 5 mg/kg, milder histopathological changes could still be observed with free DNR, but not significant with micellar formulation of DNR. No significant toxicity was detected in lungs and kidneys although the proximal tubules show somewhat ischemia damage even at 25 mg/kg of DNR.

### Drug delivery to major organs

Next, we determined whether the difference in toxicity may be secondary to the change of drug delivery. Therefore, we compared the biodistribution of DNR and its metabolites in major organs 24 h after treatment (Figure 5). To eliminate the interference of intrinsic fluorescence, organs from mice not treated with DNR were used as blank controls. Much more DNR and its metabolites were found in cardiac tissue from mice treated with free DNR ( $3.30 \pm 0.35 \mu\text{g/g}$  of tissue) when compared with the DNR concentrations from mice treated with NTM–DNR ( $1.00 \pm 0.23 \mu\text{g/g}$ ;  $p = 0.0004$ ) or CTM–DNR ( $2.05 \pm 0.49 \mu\text{g/g}$ ;  $p = 0.01$ ).



We also observed significantly increased uptake of DNR in liver and spleen that may be secondary to the uptake and clearance of micelles by the reticuloendothelial cells, but was not associated with increased toxicity as determined by liver function testing. No significant difference of DNR was observed in lung tissue among these three formulations. Even though the AUC concentration of DNR was lower with CTM–DNR than NTM–DNR in both mice and rats, the difference of DNR in other major organs was not consistently observed. At this time, it was not clear if the difference was random variations, or true delivery difference.

### Comparison of anti-tumor efficacy

We established leukemia subcutaneous xenografts from a leukemia cell line K562 expressing CLL1. Mice were treated with PBS (control), free DNR (10 mg/kg) or CTM–DNR (10 or 20 mg/kg) every 3 days for six doses. As shown in Supplementary Information 5, different formulations of DNR had significant anti-tumor effects by inhibiting the tumor growth of K562-CLL1. CTM–DNR at 20 mg/kg significantly prolonged the overall survival (more than 75 days), compared with the control (PBS, 22 days;  $p < 0.001$ ) and free DNR (44 days;  $p < 0.001$ ).

### Discussion

In this report, we evaluated the PK properties and cardiotoxicity of the CTM that can specifically target AML stem cells expressing CLL1 [8]. The improved PK profile and reduced cardiotoxicity can have dramatic clinical implication.

First, micellar formulation of DNR dramatically mitigates the cardiotoxicity. The cardiotoxicity of DNR is dose-dependent and multifactorial, which may include inhibition and/or poisoning of topoisomerase-II $\beta$  in cardiomyocytes [22], reactive oxygen species formation in the heart and interference with the ryanodine receptors of the sarcoplasmic reticulum, among others. DNR in CTM at five-times the therapeutic dose had similar cardiac toxicity as free DNR at the therapeutic dose (Figure 3C & 4A). We showed significant decrease of DNR and its metabolites in cardiac tissue when DNR was formulated in both nontargeting and CLL1-targeting micelles (Figure 5). Even though we only examined the acute toxicity up to 5 days after treatment, it has already been showed that early troponin elevations can predict longterm cardiac damage, left ventricular dysfunction and congestive heart failure from anthracyclines [23]. Therefore, we reasonably believe that micellar formulation can reduce cardiotoxicity of DNR.

Second, micellar formulation dramatically changes the PKs of DNR. Compared with free DNR, NTM–DNR and CTM–DNR significantly increased the AUC DNR concentration by 34- and 32-fold, respectively, in mice (Figure 2A). Similar changes were also observed in rats (Figure 2B). In both cases, the AUC of DNR for CTM–DNR was lower than that of NTM–DNR, mainly secondary to the initial rapid decrease from tissue distribution. It is possible that the CLL1-targeting ligand can also bind to mouse and rat CLL1 and contributed to the initial rapid clearance as the amino acid sequences are 50% identical between human and mouse CLL1 proteins, and 54% identical between human and rat CLL1 proteins. The AUC difference between free DNR and two micellar formulations of DNR

was 20–30-times while the AUC difference between CTM–DNR and NTM–DNR was approximately 25%. Therefore, we believe that the PK difference between free DNR and the micellar formulations of DNR may have dramatic therapeutic effects, but the difference between CTM and NTM is at most moderate.

In addition, decreased toxicity associated with micellar formulation allows administration of higher dose (up to three- to four-times) of DNR compared with free DNR [21]. Taking into account of decreased drug metabolism and increased drug dose, CTM can potentially increase circulating DNR concentration by more than 50-times the DNR concentration achieved by free DNR at therapeutic dose. In this study, we did not determine whether increased blood AUC DNR concentration could be translated to increased drug delivery to LSCs expressing CLL1. However, we previously showed that, at the therapeutic concentration of approximately 4  $\mu\text{M}$ , the CLL1-targeting ligand increased the micelle-mediated drug delivery to CLL1-expressing cells by approximately threefold [8]. Many *in vivo* factors may affect the actual drug delivery to cancer cells. However, unlike solid tumors that are mainly located at the extravascular space, the proximity location of LSCs and leukemia cells in blood vessels and bone marrow allows the direct contact of these cells to micelles after intravenous administration. Therefore, the dramatic change of DNR PKs by formulating in the micelles may have clinical therapeutic significance. Furthermore, because of decreased toxicity, three- to four-times the therapeutic dose of DNR can be given to AML patient. This increased dose alone can potentially kill both leukemia cells and LSCs as it has been shown that DNR at two-times the therapeutic dose can improved the overall survival [24, 25].

Micellar formulation of DNR dramatically modifies the drug distribution. DNR is a small molecule that diffuses to tissue rapidly and has large volume of distribution after intravenous administration. We showed in our study that, even though higher blood concentration of DNR was observed in mice receiving NTM or CTM, DNR concentration in some organs, including the heart, lungs and kidneys, did not increase at all. This suggests that micelles reduce the rapid diffusion, and modify the tissue distribution. This can explain the fact that the cardiac toxicity of DNR was significantly mitigated when DNR was formulated in micelles. All cardiomyocyte injury markers, including the apoptosis marker caspase 3/7 in cardiac tissue and cardiomyocyte-specific CK-MB and cTnT, significantly decreased in mice treated with DNR in micelles when compared with free DNR. This could have important clinical significance as cardiac toxicity is one of the major toxicity of DNR. Many AML patients already have cardiac diseases at the diagnosis of AML that precludes the use of DNR and other anthracyclines, one of the most powerful anti-AML drugs. High DNR concentration in livers and spleens could be secondary to clearance of nanoscale micelles by reticuloendothelial cells and was not translated into liver toxicity.

The micellar formulation of DNR has several advantages over Doxil<sup>®</sup> (Sequus Pharmaceuticals, Inc., CA, USA), a liposomal formulation of doxorubicin (or hydroxydaunorubicin) that has been in clinical application for decades. Micelles described in this project have several features for ideal nanoparticles, such as high drug-loading capacity, narrow size distribution, well-defined structure, good ‘solubility’ for hydrophobic drugs, simple multifunctionalization for cancer targeting, ease of sterilization,

straightforward manufacturing process, superior physical and chemical stability and biocompatibility. The micellar building material telodendrimers are relatively nontoxic to cells as PEG has been extensively used in drug modification for years and cholic acid is a natural component of bile. We previously showed that, during cell culture, telodendrimers were not toxic at 1 mg/ml, a concentration ten- to 100-times higher than that anticipated for clinical applications [3]. In addition, CTM has the size of around 14 nm compared with approximately 80–100 nm for Doxil. We previously showed that small-size micelles (17–60 nm) had better drug delivery to tumor sites than large ones [9]. Furthermore, as the micellar building monomer telodendrimer is synthesized through stepwise chemical synthesis, other functional groups and ligands can be added. For example, disulfide bonds can be added to synthesize crosslinked micelles that increases the stability of micelles during circulation [26]; cancer-targeting ligands can be added on the surface for cancer-specific drug delivery as in the case of CTM [8] and our bladder cancer-targeting micelles [21]. Even though both micellar formulation and Doxil favorably modify the PKs of anthracycline significantly [27], the reduction of cardiac toxicity by micellar formation seems to be much more effective than that by liposomal doxorubicin. Quantitative analyses showed that negatively charged liposome did not significantly reduce the extent and severity of cardiac toxicity, while positively charged liposomal formulation of doxorubicin reduced the cardiac toxicity by approximately twofold [28]. Our study showed that DNR in micellar formation at five-times the therapeutic dose had similar cardiac toxicity as free DNR at the therapeutic dose in both quantitative (Figure 3C) and qualitative (Figure 4A) analyses.

## Conclusion

We have successfully developed a novel nanomicellar formulation of DNR. This micellar formulation of DNR dramatically alters the PKs of DNR, increases the blood AUC of DNR, significantly decreases cardiac toxicity and increased the anti-tumor effects *in vivo*. We have previously showed that the CLL1-targeting ligand on the surface of micelles induces the targeted delivery of micelles into LSC. Therefore, increased blood DNR can potentially allow delivery of more DNR into LSC, kill this cell population and eradicate AML from the very root. As this micellar formulation decreases the cardiotoxicity, and other toxicity in general, more patients including those patients with cardiac diseases can be treated with DNR, the most effective cytotoxic drug in clinic.

## Future perspective

The prognosis of AML has not changed significantly over the last three decades. Even with the development of targeted therapy, nonspecific cytotoxic chemotherapy with the 7 + 3 regimen of cytarabine plus anthracycline is still the main treatment for AML. This regimen is associated with significant toxicity and only moderate effective with less than a third of patients being cured. In the elderly patients, less than 10% are cured. Numerous studies have showed that LSCs play critical roles in leukemogenesis in that they can self-renew, regenerate more leukemia cells and cause disease recurrence. The LSC-targeting micelles loaded with DNR can potentially deliver high-dose DNR directly into and kill LSC. Therefore, these targeting micelles can possibly increase the cure rate and improve the treatment outcomes of AML. More importantly, the micellar formulation of DNR

significantly decreases cardiotoxicity, a major and sometimes the limiting toxicity of DNR clinical use. Pharmacology and toxicology studies are being planned to support the Investigational New Drug application. It is expected this micellar formation of DNR will enter a clinical trial within the next 2–3 years. A preliminary efficacy and toxicity from a Phase II clinical trial will be obtained within the next 5–10 years.

## Supplementary Material

Refer to Web version on PubMed Central for supplementary material.

## Acknowledgments

This study was supported by the California Institute for Regenerative Medicine (CIRM) New Faculty Award (principal investigator: C-x Pan), the VA Career Development Award-2 and VA Merit (principal investigator: C-x Pan), and the National Cancer Institute Cancer Center Support Grant (principal investigator: R de Vere White and C-x Pan as a staff investigator) and Cancer Clinical Investigator Team Leadership Award (C-x Pan). KS Lam is the founder of the Lamnotherapeutics Inc., which has licensed the patent of the micellar formulation from the University of California, Davis for commercial development.

## References

1. Torchilin VP. Recent advances with liposomes as pharmaceutical carriers. *Nat. Rev. Drug Discov.* 2005; 4(2):145–160. [PubMed: 15688077]
2. Xiao K, Luo J, Fowler WL, et al. A self-assembling nanoparticle for paclitaxel delivery in ovarian cancer. *Biomaterials.* 2009; 30(30):6006–6016. [PubMed: 19660809]
3. Li Y, Xiao K, Luo J, Lee J, Pan S, Lam KS. A novel size-tunable nanocarrier system for targeted anticancer drug delivery. *J. Control. Release.* 2010; 144(3):314–323. [PubMed: 20211210]
4. Lee CC, Mackay JA, Frechet JM, Szoka FC. Designing dendrimers for biological applications. *Nat. Biotechnol.* 2005; 23(12):1517–1526. [PubMed: 16333296]
5. Andreopoulou E, Gaiotti D, Kim E, et al. Pegylated liposomal doxorubicin HCL (PLD; Caelyx/Doxil): experience with long-term maintenance in responding patients with recurrent epithelial ovarian cancer. *Ann. Oncol.* 2007; 18(4):716–721. [PubMed: 17301073]
6. Berry G, Billingham M, Alderman E, et al. The use of cardiac biopsy to demonstrate reduced cardiotoxicity in AIDS Kaposi's sarcoma patients treated with pegylated liposomal doxorubicin. *Ann. Oncol.* 1998; 9(7):711–716. [PubMed: 9739435]
7. Safra T, Muggia F, Jeffers S, et al. Pegylated liposomal doxorubicin (doxil): reduced clinical cardiotoxicity in patients reaching or exceeding cumulative doses of 500 mg/m<sup>2</sup>. *Ann. Oncol.* 2000; 11(8):1029–1033. [PubMed: 11038041]
8. Zhang H, Luo J, Li Y, et al. Characterization of high-affinity peptides and their feasibility for use in nanotherapeutics targeting leukemia stem cells. *Nanomedicine.* 2012; 8(7):1116–1124. [PubMed: 22197725]
9. Luo J, Xiao K, Li Y, et al. Well-defined, size-tunable, multifunctional micelles for efficient paclitaxel delivery for cancer treatment. *Bioconjug. Chem.* 2010; 21(7):1216–1224. [PubMed: 20536174]
10. van Rhenen A, van Dongen GA, Kelder A, et al. The novel AML stem cell associated antigen CLL-1 aids in discrimination between normal and leukemic stem cells. *Blood.* 2007; 110(7):2659–2666. [PubMed: 17609428]
11. Bakker AB, van den Oudenrijn S, Bakker AQ, et al. C-type lectin-like molecule-1: a novel myeloid cell surface marker associated with acute myeloid leukemia. *Cancer Res.* 2004; 64(22):8443–8450. [PubMed: 15548716]
12. Bonnet D, Dick JE. Human acute myeloid leukemia is organized as a hierarchy that originates from a primitive hematopoietic cell. *Nat. Med.* 1997; 3(7):730–737. [PubMed: 9212098]

13. Sutherland HJ, Blair A, Zapf RW. Characterization of a hierarchy in human acute myeloid leukemia progenitor cells. *Blood*. 1996; 87(11):4754–4761. [PubMed: 8639846]
14. Pan CX, Zhu W, Cheng L. Implications of cancer stem cells in the treatment of cancer. *Future Oncol*. 2006; 2(6):723–731. [PubMed: 17155899]
15. Terpstra W, Ploemacher RE, Prins A, et al. Fluorouracil selectively spares acute myeloid leukemia cells with long-term growth abilities in immunodeficient mice and in culture. *Blood*. 1996; 88(6): 1944–1950. [PubMed: 8822911]
16. Copland M, Hamilton A, Elrick LJ, et al. Dasatinib (BMS-354825) targets an earlier progenitor population than imatinib in primary CML but does not eliminate the quiescent fraction. *Blood*. 2006; 107(11):4532–4539. [PubMed: 16469872]
17. McDonagh CF, Huhlov A, Harms BD, et al. Antitumor activity of a novel bispecific antibody that targets the ErbB2/ErbB3 oncogenic unit and inhibits heregulin-induced activation of ErbB3. *Mol. Cancer Ther*. 2012; 11(3):582–593. [PubMed: 22248472]
18. Chan, WC.; White, PD. *Fmoc Solid Phase Peptide Synthesis : a Practical Approach*. Oxford, UK: Oxford University Press; 2000.
19. Gabriëlsson J, Weiner D. Non-compartmental analysis. *Methods Mol. Biol*. 2012; 929:377–389. [PubMed: 23007438]
20. Cortes J, Estey E, O'Brien S, et al. High-dose liposomal daunorubicin and high-dose cytarabine combination in patients with refractory or relapsed acute myelogenous leukemia. *Cancer*. 2001; 92(1):7–14. [PubMed: 11443603]
21. Lin TY, Li YP, Zhang H, et al. Tumor-targeting multifunctional micelles for imaging and chemotherapy of advanced bladder cancer. *Nanomedicine (Lond.)*. 2012; 8:1239–1251. [PubMed: 23199207]
22. Zhang S, Liu X, Bawa-Khalfe T, et al. Identification of the molecular basis of doxorubicin-induced cardiotoxicity. *Nat. Med*. 2012; 18(11):1639–1642. [PubMed: 23104132]
23. Cardinale D, Sandri MT, Martinoni A, et al. Myocardial injury revealed by plasma troponin I in breast cancer treated with high-dose chemotherapy. *Ann. Oncol*. 2002; 13(5):710–715. [PubMed: 12075738]
24. Fernandez HF, Sun Z, Yao X, et al. Anthracycline dose intensification in acute myeloid leukemia. *N. Engl. J. Med*. 2009; 361(13):1249–1259. [PubMed: 19776406]
25. Lowenberg B, Ossenkoppele GJ, van Putten W, et al. High-dose daunorubicin in older patients with acute myeloid leukemia. *N. Engl. J. Med*. 2009; 361(13):1235–1248. [PubMed: 19776405]
26. Li Y, Xiao K, Luo J, et al. Well-defined, reversible disulfide cross-linked micelles for on-demand paclitaxel delivery. *Biomaterials*. 2011; 32(27):6633–6645. [PubMed: 21658763]
27. Rahman A, Carmichael D, Harris M, Roh JK. Comparative pharmacokinetics of free doxorubicin and doxorubicin entrapped in cardiolipin liposomes. *Cancer Res*. 1986; 46(5):2295–2299. [PubMed: 3697976]
28. Rahman A, More N, Schein PS. Doxorubicin-induced chronic cardiotoxicity and its protection by liposomal administration. *Cancer Res*. 1982; 42(5):1817–1825. [PubMed: 7066898]

### Executive summary

#### Pharmacokinetics of micellar formulation of daunorubicin

- Both nontargeting and CLL1-targeting micelles loaded with daunorubicin (DNR) significantly prolong the half-life of DNR by more than 15-times of free DNR.
- Micellar formation of DNR increases the area under the concentration curve of DNR by more than 30-times in mice and 20-times in rats when compared with free DNR.

#### Cardiac toxicity of micellar formulation of DNR

- Micellar formulations of DNR significantly decrease the cardiac toxicity as measured by plasma cardiac damage markers creatine kinase MB isoenzyme and cardiac troponin.
- The apoptosis marker caspase 3/7 levels are comparable in the cardiac tissues from mice treated with control or CLL1-targeting micelles-DNR at five-times the therapeutic dose.
- At the same dose level, DNR in micellar formulations induces much milder histopathological changes than free DNR.
- Decreased cardiac toxicity may be related to decreased DNR drug delivery to cardiac tissue of the micellar formations.

#### Toxicity & drug delivery to other organs

- Significant histopathological changes can be observed in liver and spleen with free DNR at 5 (therapeutic dose) and 25 mg/kg of free DNR, but much milder with micellar formations of DNR even at 25 mg/kg.
- No significant toxicity in lung or kidney is observed with free or micellar formulations of DNR at 5 and 25 mg/kg.

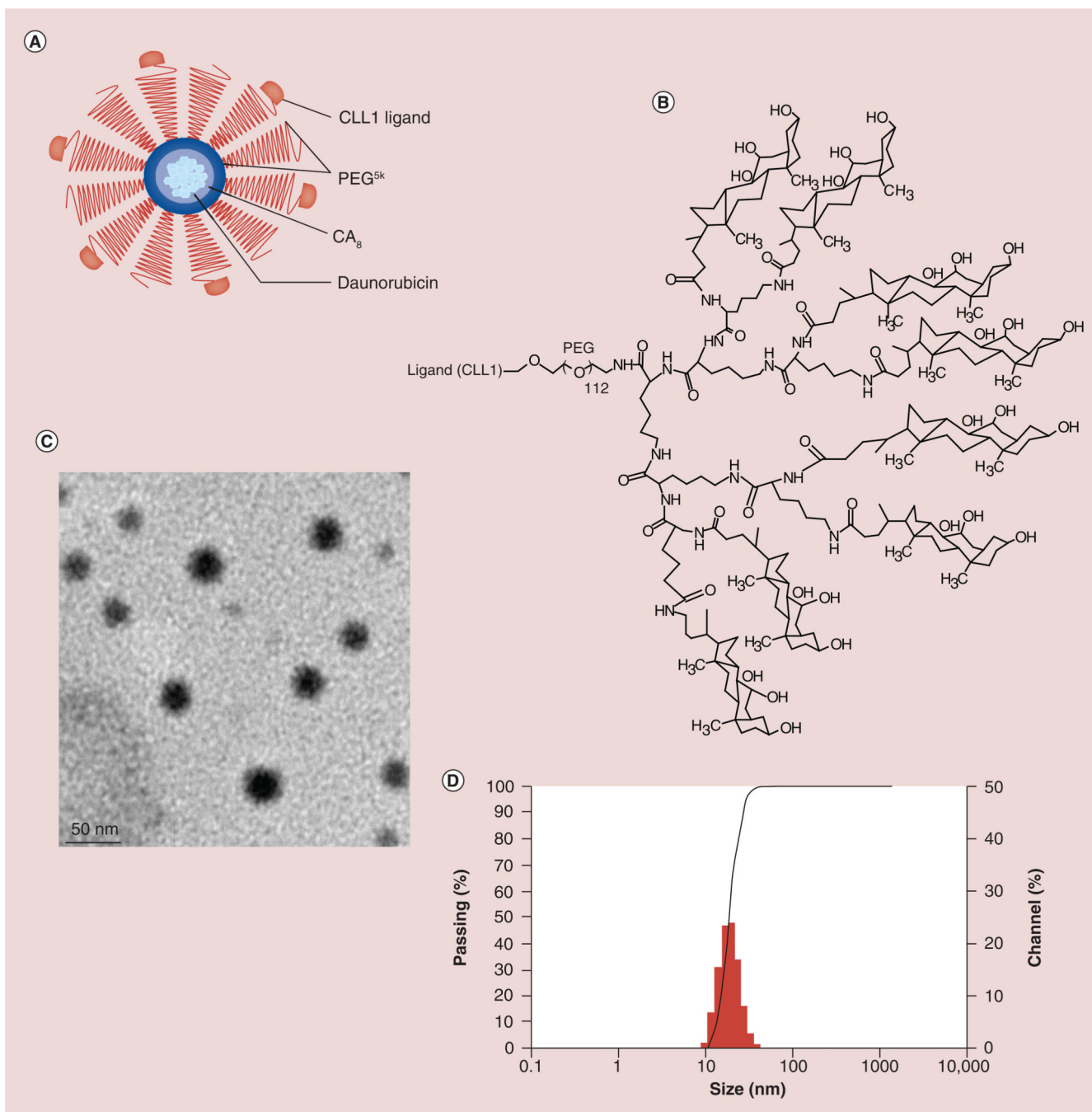


### Figure 1. Characterization of CLL1-targeting micelles

(A) Schematic diagram of CLL1-targeting micelles (CTM). (B) The chemical structure of CLL1-L-telodendrimer. Telodendrimer PEG<sup>5K</sup>-CA<sub>8</sub> represents PEG with the molecular weight of 5000 Da (PEG<sup>5K</sup>) conjugated with eight cholic acid subunits at one terminus. To synthesize CTM, CLL1-L is conjugated at the other terminus of PEG in telodendrimers. Cholic acid is an amphiphilic molecule with the hydrophobic methyl groups at one side and hydrophilic hydroxyl groups at the other side. This facial amphiphilic structure allows the formation of hydrophobic spheric micelle core to load daunorubicin while leaving

hydrophilic PEG and CLL1-L displayed on the surface for targeted drug delivery. Each CTM contains approximately 100–200 telodendrimers. The data presented below were obtained with CTM in which 50% of telodendrimers are conjugated with CLL1-L. **(C)** The size of CTM–daunorubicin as observed by transmission electron microscopy. **(D)** The size of CTM loaded with daunorubicin was approximately 14 nm with a narrow size distribution, as determined by dynamic light scattering.

**(B)** PEG: Polyethylene glycol.



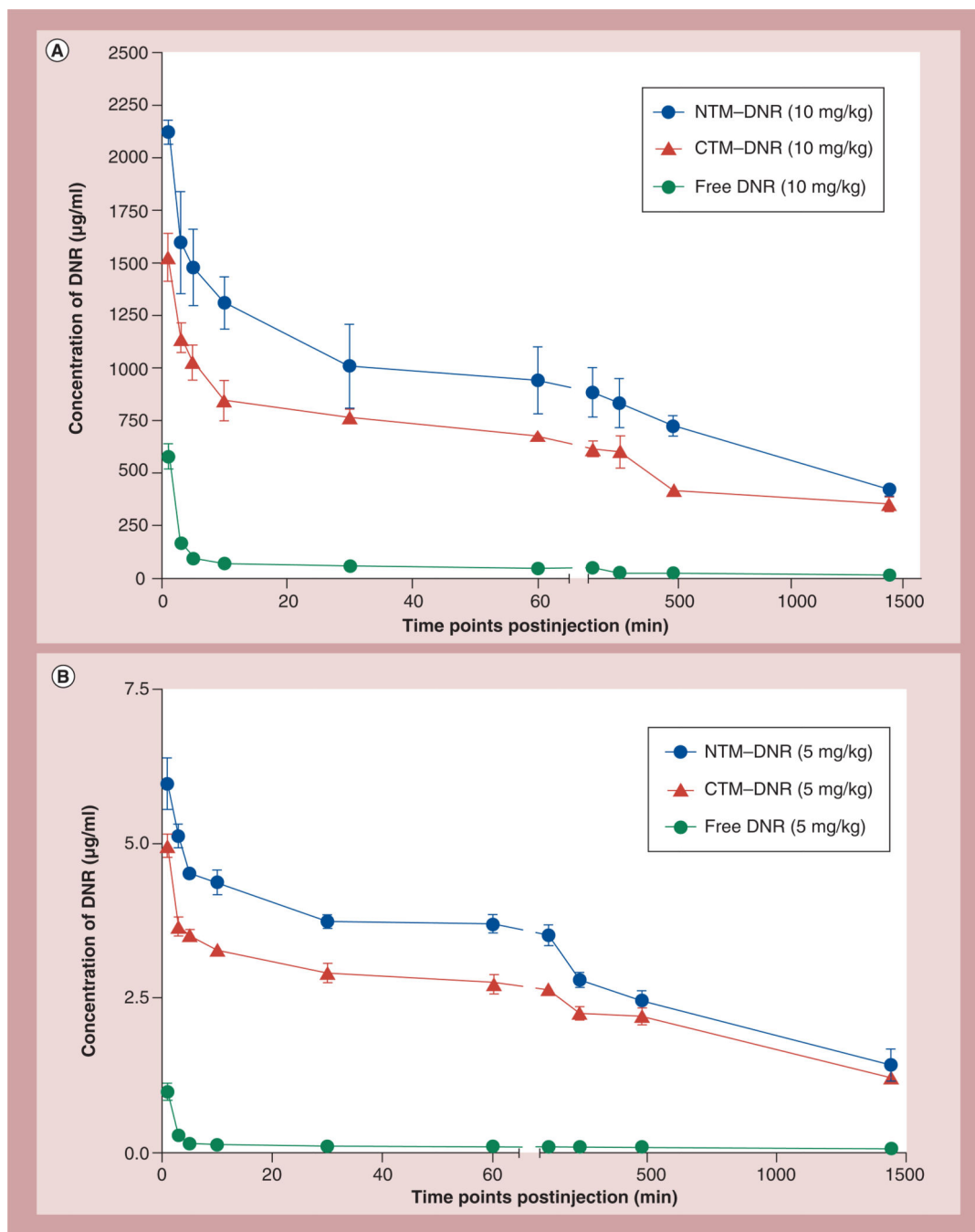


**Figure 2. Pharmacokinetic studies of free daunorubicin, nontargeting micelles–daunorubicin and CLL1-targeting micelles–daunorubicin**

(A) Pharmacokinetics of DNR in mice. (B) Pharmacokinetics of DNR in rats. All three formulations of DNR had a fast first-phase decrease of DNR, followed by slower clearance of DNR. The area under curve from 0 to 24 h for NTM–DNR and CTM–DNR were 33.9-fold ( $p < 0.001$ ) and 31.9-fold ( $p = 0.002$ ) greater than free DNR in mice, and 25.0-fold ( $p = 0.0056$ ) and 22.0-fold ( $p = 0.0009$ ) higher than free DNR in rats. However, the area under

curve from 0 to 24 h difference between NTM–DNR and CTM–DNR was not statistically significant (0.43 in mice and 0.25 in rats).

CTM: CLL1-targeting micelles; DNR: Daunorubicin; NTM: Nontargeting micelles–daunorubicin.

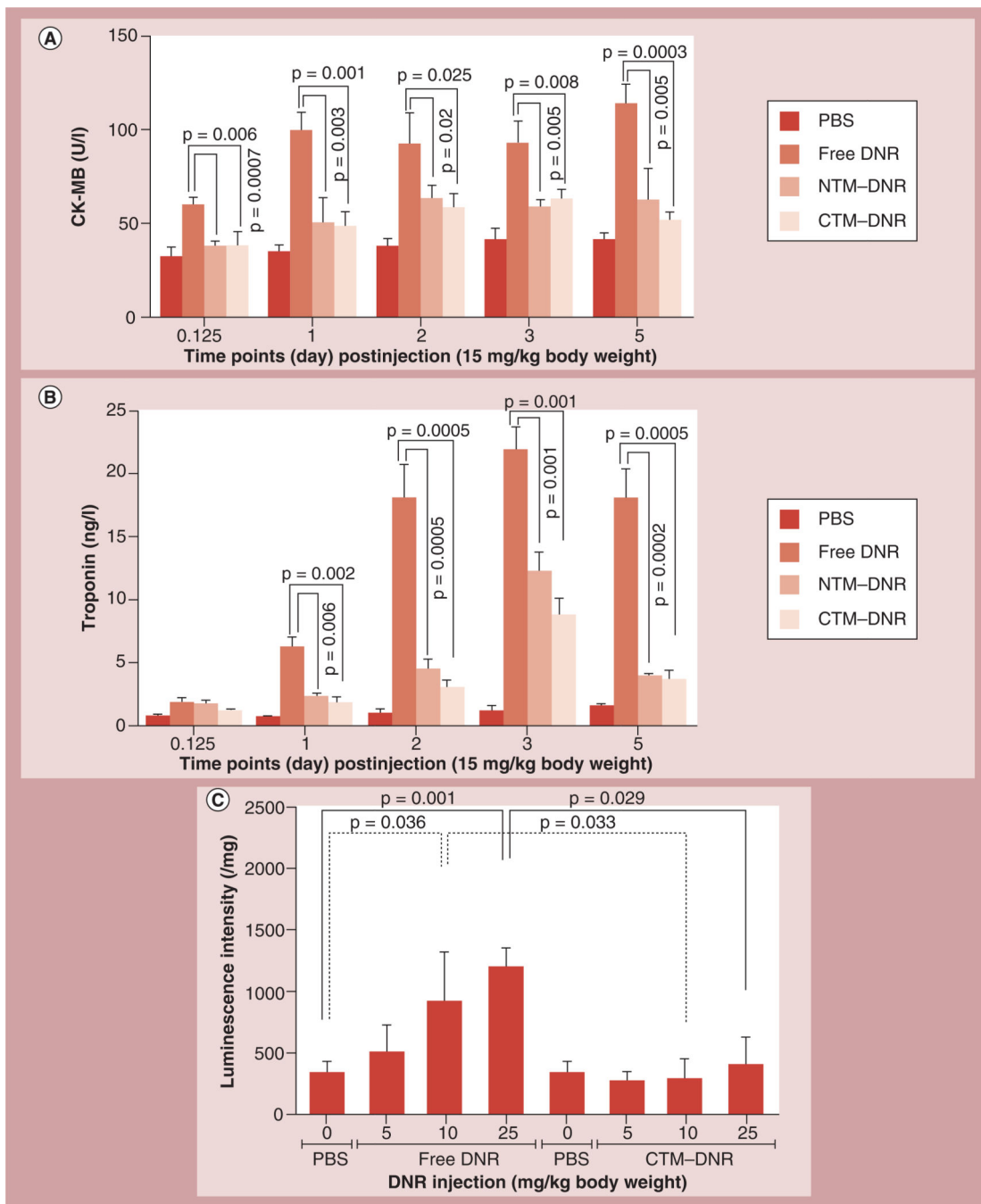


**Figure 3. Changes of cardiac damage markers**

Blood specimens were collected after a single injection of different drugs with the DNR dose at 15 mg/kg body weight. (A) CK-MB isoenzyme levels in plasma. (B) Troponin levels in plasma. The CK-MB isoenzyme (A) and troponin (B) levels were significantly higher after injection of free DNR compared with the control or NTM-DNR and CTM-DNR treatment. (C) Caspase 3/7 induction in cardiac tissues. The heart tissues from mice 5 days after treatment with DNR and CTM-DNR were homogenized, lysed and then the activity of caspase 3/7 was measured. Compared with controlled mice, there was a dose-dependent

induction of the caspase 3/7 activity in heart tissues in the mice treated with free DNR, while no significant induction was observed in the mice treated with CTM–DNR at the same dose range.

CK-MB: Creatine kinase MB; CTM: CLL1-targeting micelles; DNR: Daunorubicin; NTM: Nontargeting micelles–daunorubicin; PBS: Phosphate-buffered saline.

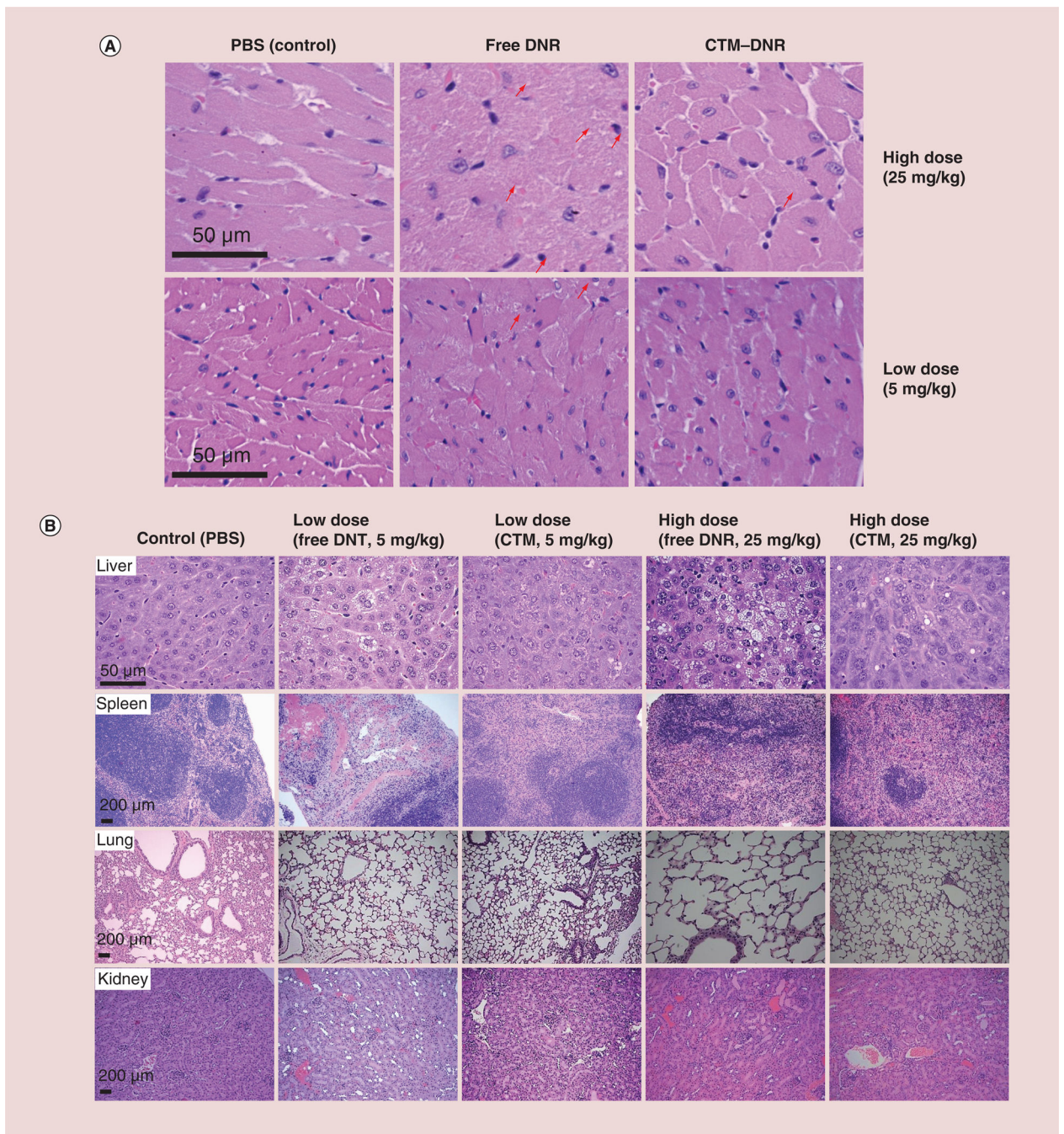


#### Figure 4. Histopathologic changes of vital organs

All organs were obtained 5 days after treatment. **(A)** The histology of the heart tissue. Heart tissue from mice treated with free DNR at 5 and 25 mg/kg showed marked myocardial toxicity characterized as disarray of cardiomyocytes, disruption or loss of myofibrils (arrows pointing to the example cells) and vacuolization of the cytoplasm, and inflammatory cells. When mice were treated with CTM-DNR at 25 mg/kg, only occasional myofibril disruption was observed (arrow). **(B)** Histological observation in other organs. Significant histological changes were found in livers and spleen from those mice treated with low- (5 mg/kg) and

high-dose (25 mg/kg) groups of free DNR. Similar, but much less, toxicity was observed in these two organs when mice received DNR micelles. Less toxicity was also observed in spleen from mice treated with nanomicellar formulation. No significant changes were found in kidneys and lungs from different groups.

CTM: CLL1-targeting micelles; DNR: Daunorubicin; PBS: Phosphate-buffered saline.

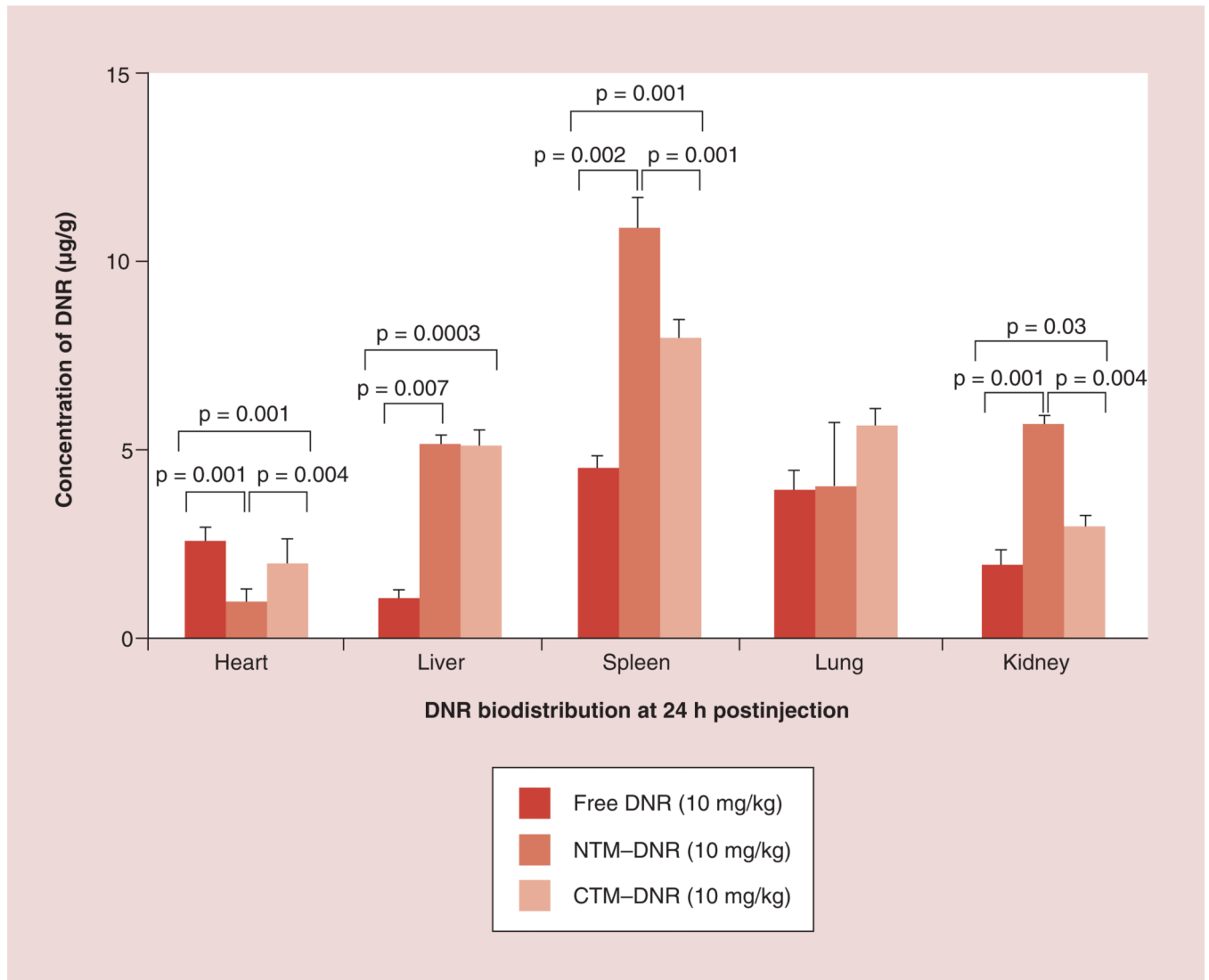


**Figure 5. Drug delivery to vital organs**

Micellar formulation of DNR had significant less DNR delivery to heart tissue, but more to liver and spleen.

CTM: CLL1-targeting micelles; DNR: Daunorubicin; NTM: Nontargeting micelles–daunorubicin.

Table 1

The pharmacokinetic parameters of free daunorubicin and daunorubicin micellar formulations.

| Parameters  | Free DNR       | NTM-DNR        | CTM-DNR        | p-value <sup>†</sup> |
|---|----------------|----------------|----------------|----------------------|
|   | Mean ± SD      | Mean ± SD      | Mean ± SD      |                      |
| <b>Mice</b>   |                |                |                |                      |
| $\alpha$ (min <sup>-1</sup> )                                       | 0.63 ± 0.02    | 0.14 ± 0.07    | 0.08 ± 0.06    | 0.0001               |
| $\beta$ (min <sup>-1</sup> )  | 0.0001         | 0              | 0.00 ± 0.00    | 0.004                |
| AUC <sub>0-t</sub><br>( $\mu\text{g} \times \text{h}^2/\text{ml}$ ) | 836 ± 151      | 28,333 ± 833   | 26,667 ± 6333  | <0.001               |
| MRT (h)   | 1002 ± 79      | 1648 ± 209     | 2682 ± 860     | 0.004                |
| C <sub>max</sub> calc   | 961 ± 92       | 2157 ± 221     | 1386 ± 121     | 0.0005               |
| Kel   | 3.68 ± 6.35    | 0.00 ± 0.00    | 0.00 ± 0.00    | 0.186                |
| T <sub>1/2<math>\alpha</math></sub> (min)                           | 1.11 ± 0.04    | 5.93 ± 2.76    | 11.63 ± 6.37   | 0.02                 |
| T <sub>1/2<math>\beta</math></sub> (h)                              | 11.9 ± 1       | 20.5 ± 3       | 31.2 ± 10      | 0.005                |
| T <sub>1/2kel</sub> (h)   | 0.61 ± 0.01    | 9.08 ± 0.4     | 13.9 ± 4.15    | <0.001               |
| V <sub>ss</sub> (ml/kg)   | 205.39 ± 47.95 | 10.45 ± 1.41   | 16.10 ± 1.58   | 0.002                |
| Cl (ml/min/kg)  | 0.20 ± 0.03    | 0.01 ± 0.00    | 0.01 ± 0.001   | 0.0003               |
| <b>Rats</b>   |                |                |                |                      |
| $\alpha$ (min <sup>-1</sup> )                                       | 0.74 ± 0.00    | 0.16 ± 0.02    | 0.29 ± 0.06    | 0.0002               |
| $\beta$ (min <sup>-1</sup> )  | 0.00 ± 0.00    | 0.00 ± 0.00    | 0.00 ± 0.00    | 0.0675               |
| AUC <sub>0-t</sub><br>( $\mu\text{g} \times \text{h}^2/\text{ml}$ ) | 3.60 ± 0.79    | 90.08 ± 13.05  | 79.22 ± 4.43   | 0.0056               |
| MRT (h)   | 36.23 ± 6.51   | 24.44 ± 3.70   | 27.65 ± 2.29   | 0.0778               |
| C <sub>max</sub> calc   | 1.91 ± 0.26    | 6.14 ± 0.30    | 5.40 ± 0.01    | 0.0021               |
| Kel   | 0.01 ± 0.00    | 0.00 ± 0.00    | 0.00 ± 0.00    | 0.0008               |
| T <sub>1/2<math>\alpha</math></sub> (min)                           | 0.94 ± 0.00    | 4.45 ± 0.47    | 2.45 ± 0.55    | 0.0045               |
| T <sub>1/2<math>\beta</math></sub> (h)                              | 25.40 ± 4.54   | 16.99 ± 2.58   | 19.20 ± 1.60   | 0.0751               |
| T <sub>1/2kel</sub> (h)   | 2.01 ± 1.12    | 10.14 ± 0.99   | 10.17 ± 0.54   | 0.0082               |
| V <sub>ss</sub> (ml/kg)   | 50,836 ± 1659  | 1355.61 ± 8.98 | 1743.91 ± 47.1 | 0.0003               |



| Parameters     | Free DNR     |                      | NTM-DNR     |                      | CTM-DNR     |                      | p-value <sup>†</sup> |
|----------------|--------------|----------------------|-------------|----------------------|-------------|----------------------|----------------------|
|                | Mean ± SD    | p-value <sup>‡</sup> | Mean ± SD   | p-value <sup>‡</sup> | Mean ± SD   | p-value <sup>§</sup> |                      |
| Cl (ml/min/kg) | 23.73 ± 5.20 | 0.93 ± 0.14          | 0.93 ± 0.14 | 0.0125               | 1.05 ± 0.06 | 0.0126               | 0.187                |

<sup>†</sup> Comparison of NTM-DNR and CTM-DNR.

<sup>‡</sup> Comparison of free DNR and NTM-DNR.

<sup>§</sup> Comparison of free DNR and CTM-DNR.

α: Exponent<sub>kel</sub>, elimination rate constant from central compartment; β: Exponent<sub>t1/2α</sub> (min), elimination half-life of α; AUC<sub>0-24h</sub>: Area under curve from 0 to 24 h; AUMC: Partial area under the moment curve; Cl: Clearance from the blood; C<sub>max</sub> calc: Peak plasma concentration of a drug; CTM: CLL1-targeting micelles; DNR: Daunorubicin; MRT: Mean residence time; NTM: Nontargeting micelles-daunorubicin; SD: Standard deviation; T<sub>1/2β</sub>: Elimination half-life of β; T<sub>1/2kel</sub>: Overall half-life; V<sub>ss</sub>: Steady-state volume of distribution.